Supplementary Table 1. **Clinically relevant variants and polymorphisms in the BK channel that cause intellectual disability**

Variant	Sequence context	Effect on channel	Clinical Phenotype	In structure	Reference and accession codes (where reported)
A138V	INNGSSQ**A**DG	Patient cells showed reduced activity of a K+ channel Small variable effect on currents in transfected HEK cells.	Severe ID, epilepsy, and autism spectrum disorder	**no**	Laumonnier 2006 Given as NM_002227 (possibly a misprint as this is Janus Kinase) probably NM_002247 Plante et al., 2019 MG279688
S351Y	ECVYLLMVTM **S**TVGYGDVYA	LoF abolished BK current.	Mild ID	**yes**	Liang et al., 2019 NM_002247.3
G354S	STV**G**YGDVYA	LoF When expressed by adenovirus in cerebellum rescued by NS1619.	ID with cerebellar ataxia Loss of mitochondrial function. Chlorzoxazone (BK/SK activator) gave partial improvement.	**yes**	Du et al., 2020 NM_002247
C413Y	VV**C**GHITLES	Partial LoF	mild to severe ID, speech delay, ataxia, axial hypotonia, and cerebral atrophy	**yes**	Liang et al., 2019 NM_002247.3
N449fs	VFLHNISP**N**L	Frame shift. LoF.	ID not reported but mild cerebellar atrophy	**yes**	Liang et al., 2019 NM_002247.3
N599D	KYYLEGVS**N**E MYTEYLSSAF	Possible LoF as does not facilitate opening	Not reported	**yes**	Plante et al., 2019 MG279688
I663V	HLKIQEGTLG FF**I**ASDAKEV	LoF abolishes BK current	ID, hypotonia, ataxia	**yes**	Liang et al., 2019 NM_002247.3
Y676L-fs	KRAFF**Y**CKAC	loss of function	GDD, epilepsy, severe cerebellar atrophy	**yes**	Tabarki et al., 2016. NM_001161352.1 Liang et al.,2019 NM_002247.3
R858W	SSALIGL**R**NL	LoF.		**no**	Plante et al., 2019 MG279688
P805L also described as P840L (P863L in reference	VM**P**LRASNFH	LoF, reduction in the amplitude of the BK current and a shift to a	ID	**yes**	Bailey et al., 2020 NM_002247.3

sequence)		positive potential for the activation curve			
D1008N listed as D984N in Liang 2019	IITELVN**D**TN	LoF, marked reduction in activation of the BK channel	Moderate ID	**yes**	Liang et al., 2019 NM_002247.3
D434G	KDR**D**DVNVEI	GoF	generalized epilepsy and paroxysmal dyskinesia	**yes**	Du et al., 2005 NM_002247
C495G	ANKY**C**ADPDA	GoF, shifts $V_{1=2}$ to more hyperpolarized potentials (by -15 to -20 mV)	Not reported	**yes**	Plante et al., 2019 MG279688
N536H	KAHLL**N**IPSW	GoF	ID, dystonia. Autism spectrum disorder.	**yes**	Zhang et al. 2020
K457E	ELEALF**K**RHF	Possible GoF as treatment of the patient with 3,4-diaminopyridine was successful.	Paroxysmal dyskinesia, ataxia.	**yes**	Buckley et al. 2020 NM_001161352.2
R458ter	ELEALFK**R**HF	Truncating variant. LoF AND GoF	ID, epilepsy, corticospinal-cerebellar tract atrophy, and paroxysmal dyskinesia.	**yes**	Yesil et al. 2018 NM_001161353
E884K	GSI**E**YLKREW	Not reported	GDD and paroxysmal non-kinesigenic dyskinesia	**yes**	Zhang Z. B. et al., 2015.
N1053S	YF**N**DNILTLI	Not reported	GDD and paroxysmal non-kinesigenic dyskinesia	**yes**	Zhang Z. B. et al., 2015. Moldenhauer 2020 MG279689.1 Du et al., 2005 NM_002247

Reference sequence used was Q12791-1 (NM_002247.4), ID, intellectual disability; LoF, loss of function; GoF, gain of function. N995S, N999S, and N1053S same amino acid substitution reported in the literature as at least three different reference sequencing number schemes, sequence context is shown for clarity.

Bailey CS, Moldenhauer HJ, Park SM, Keros S, Meredith AL. *KCNMA1*-linked channelopathy. J Gen Physiol. 2019 Oct 7;151(10):1173-1189.

Buckley C, Williams J, Munteanu T, *et al*. Status Dystonicus, Oculogyric Crisis and Paroxysmal Dyskinesia in a 25 Year-Old Woman with a Novel *KCNMA1* Variant, K457E. *Tremor Other Hyperkinet Mov (N Y)*. 2020;10:49.

Du X, Carvalho-de-Souza JL, Wei C, *et al*. Loss-of-function BK channel mutation causes impaired mitochondria and progressive cerebellar ataxia. *Proc Natl Acad Sci U S A*. 2020 Mar 17;117(11):6023-6034.

Liang L, Li X, Moutton S, Schrier Vergano SA, *et al*. De novo loss-of-function KCNMA1 variants are associated with a new multiple malformation syndrome and a broad spectrum of developmental and neurological phenotypes. *Hum Mol Genet*. 2019;28(17):2937-2951.

Moldenhauer HJ, Matychak KK, Meredith AL. Comparative gain-of-function effects of the KCNMA1-N999S mutation on human BK channel properties. *J Neurophysiol*. 2020;123(2):560-570.

Plante AE, Lai MH, Lu J, Meredith AL. Effects of Single Nucleotide Polymorphisms in Human KCNMA1 on BK Current Properties. *Front Mol Neurosci*. 2019 Dec 3;12:285.

Tabarki B, AlMajhad N, AlHashem A, Shaheen R, Alkuraya FS. Homozygous KCNMA1 mutation as a cause of cerebellar atrophy, developmental delay and seizures. *Hum Genet*. 2016;135(11):1295-1298.

Yeşil G, Aralaşmak A, Akyüz E, *et al*. Expanding the Phenotype of Homozygous *KCNMA1* Mutations; Dyskinesia, Epilepsy, Intellectual Disability, Cerebellar and Corticospinal Tract Atrophy. *Balkan Med J*. 2018;35(4):336-339.

Zhang, G., Gibson, R.A., McDonald, M., *et al.* (2020), A Gain-of-Function Mutation in *KCNMA1* Causes Dystonia Spells Controlled With Stimulant Therapy. *Mov Disord*. 35:1868-1873.

Zhang ZB, Tian MQ, Gao K, Jiang YW, Wu Y. De novo KCNMA1 mutations in children with early-onset paroxysmal dyskinesia and developmental delay. *Mov Disord*. 2015 Aug;30(9):1290-2.

Supplementary Figure 1. Cellular expression of BK channel subunits in mouse brain

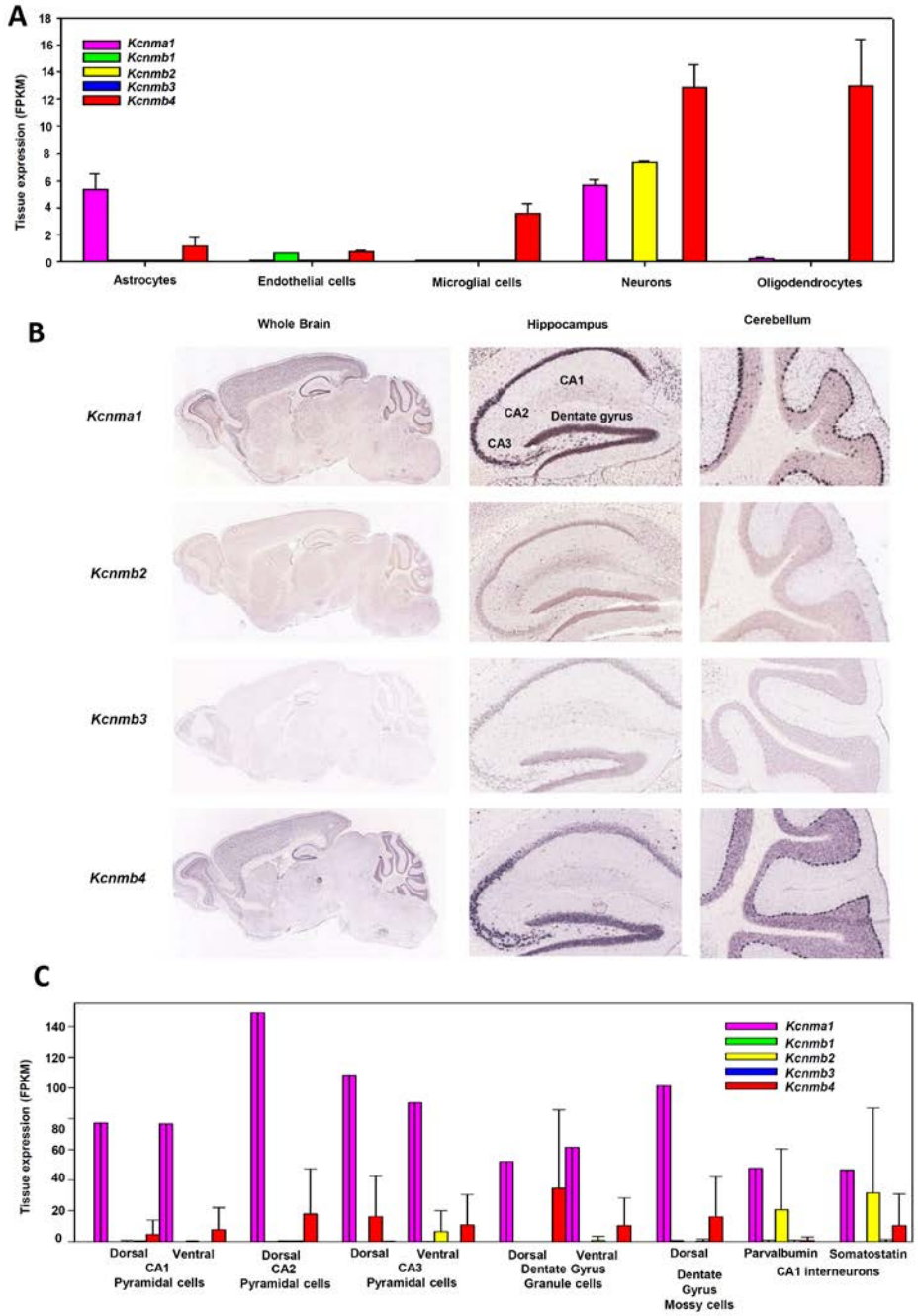

Supplementary Figure 1. Expression of BK isotypes in mouse brain. (**A**) RNAseq data was extracted from the BrainRNAseq portal for the BK isotypes. Results expressed as mean ± standard deviation for tissue expression as fragments per kilobase of transcript per million mapped reads (FPKM). (**B**) *In situ* hybridisation of BK isotypes in sagittal adult mouse brain sections reproduced from the Allen Mouse Brain Atlas showing expression of:
Kcnma1 (https://mouse.brain-map.org/experiment/show?id=74578206),
Kcnmb2 (https://mouse.brain-map.org/experiment/show?id=74635689),
Kcnmb3 (https://mouse.brain-map.org/experiment/show?id=81600586)

Kcnmb4 (https://mouse.brain-map.org/experiment/show?id=70593143)

(**C**) The expression BK subtypes in neuronal cells within the hippocampus. The results were extracted from the Hippocampus RNA-seq atlas and represent the mean and upper 95% confidence interval expressed as (FPKM) from 100 cells and 3 samples per group.

Supplementary Figure 2. Regional distribution and neuronal type of Fmr1 and BK channel subunits in mouse and human brain

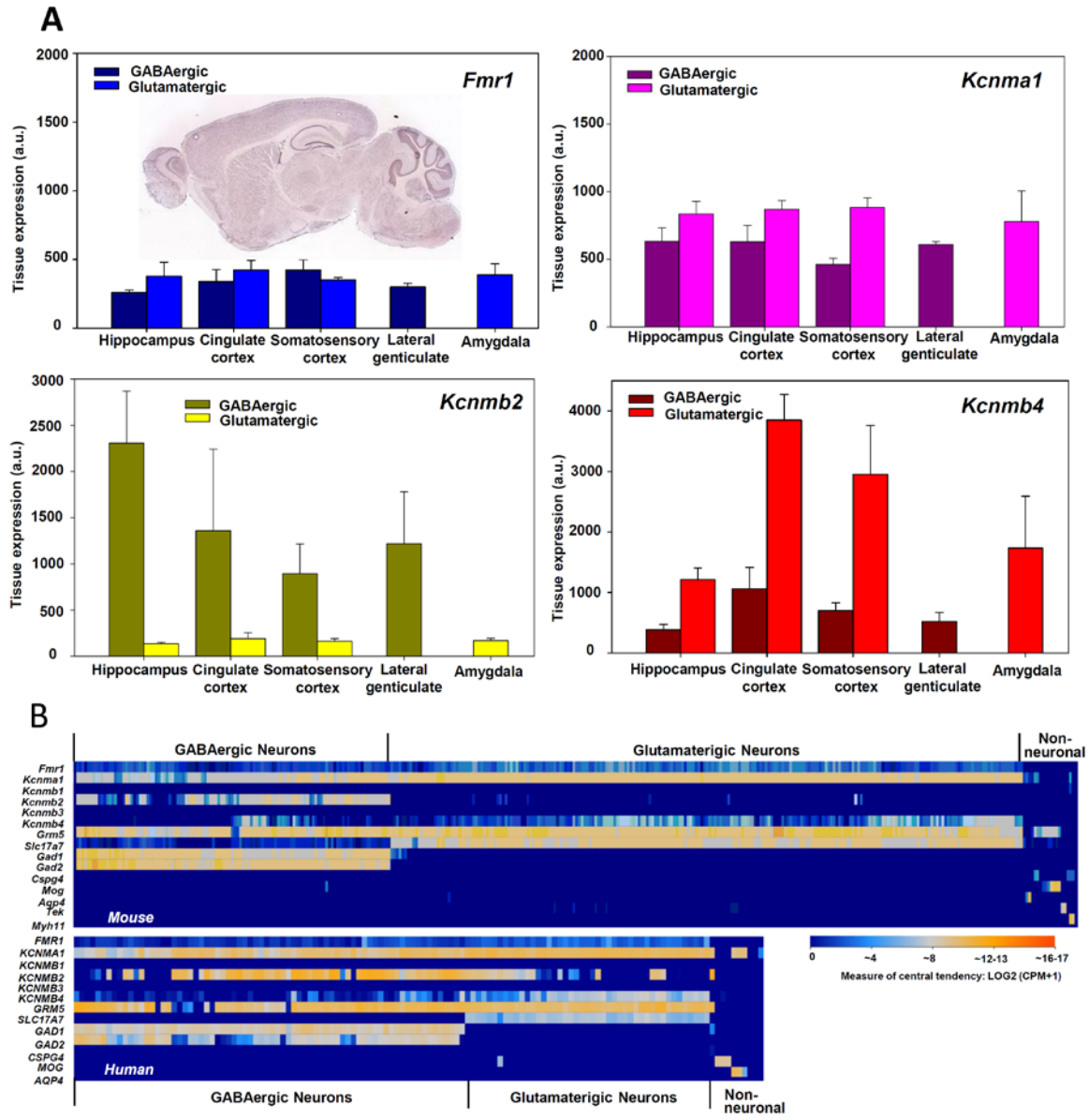

Supplementary Figure 2. Differential expression of BK isotypes in glutamatergic and GABAergic neurons. RNAseq data was extracted from: (**A**) GEO profile. The results represent the mean and standard deviation of (n = 3-9/group) for the message for FMRP and the BK subtypes for glutamatergic and GABAergic neurons. The insert demonstrates *in situ* hybridization of *Fmr1* anti-sense in mouse brain extracted from the Allen brain Atlas (http://mouse.brain-map.org/experiment/show/73606703) (**B**) 10X RNAseq data from adult mouse cortex and hippocampus and human M1 cortex samples using the Allen Brain Map Transcriptomic explorer. The results represent a heatmap of cells grouped into transcriptomic cell types for: FMRP (*Fmr1*), BK channel subunits, metabotropic glutamate receptor 5

(*Grm5*), vesicular glutamate transporter (*Slc17a7*) to detect glutamatergic cells, glutamic acid decarboxylase (*Gad*) one and two to detect GABAergic cells, NG2 chondroitin sulphate proteoglycan 4 (*Cspg4*) to detect oligodendrocyte precursors cells, myelin oligodendrocyte glycoprotein (*Mog*) to detect mature oligodendrocytes, aquaporin 4 (*Aqp4*) to detect astrocytes, endothelial tyrosine kinase (*Tek*) and myosin eleven (*Myh11*) to detect smooth muscle cells.

Supplementary Figures 1 and 2 narrative

Extraction of cell type specific RNAseq data (www.brainrnaseq.org) indicated that *Fmr1* message was notably expressed in mouse: astrocytes (58.9 ± 5.8 FPKM), neurons (13.8± 1.2 FPKM), endothelia (9.7± 0.2) and oligodendrocytes 3.4 ± 0.3 (FPKM) with low levels in microglia (1.3 ± 0.3). In rodents the *Kcnmb1* was largely restricted to the vasculature, consistent with known expression of KCNMB1 protein in smooth muscle within arteries (Baker et al. 2017. Figure 2A, Figure 3B). There was essentially no expression in neurons (Figure 2A, Figure 3B). Astrocytes expressed the BK channel alpha pore but there was limited astrocytic beta chain expression (Figure 2A, Figure 3B). These cells expressed the small conductance potassium channel KCNNR3 (www.brainrnaseq.org). Oligodendrocytes expressed KCNMB4 in rodents and humans (Figure 2A, Figure 3B), whereas oligodendrocyte precursors notably expressed KCNMA1 and KCNMB2 that was downregulated as they matured and developed KCNMB4 (Figure 3B). KCNMB3 was poorly expressed in the CNS (Figure 2A-C. Figure 3B).

As expected, the KCNMB4 isoform was associated with neural expression (Figure 2A-C, Figure 3A, B], although KCNMB2 was also present on neurons (Figure 2A-C, Figure 3A, B). *In situ* hybridisation demonstrated expression of *Kcnmb4* throughout the cortex and at high levels in the hippocampus and cerebellum (Figure 2B). This was confirmed in RNAseq data of the hippocampus with higher levels in the CA2 and CA3 regions (Figure 2C). In the hippocampus there was a low level of KCNMB2 expression except in the somatostatin (Sst) and parvalbumin (Pavalb) interneurons (Figure 2C). These were typically inhibitory, gamma aminobutyric acid (GABA) secreting neurons and suggested that KCNMB2 may be more prominent on GABAergic cells. Indeed, this was supported in microarray and RNAseq data in rodents (Figure 3A, 3B) and to some extent in humans (Figure 3B). *Fmr1* was detected throughout the brain (Figure 3A) on both GABAergic and glutamatergic neurons (Figure 3A), although some glutamatergic brain cells seemed to express high levels (Figure 3B). It

appeared that *Kcnmb4* and KCNMB4 was preferentially expressed by glutamatergic neurons in a variety of brain structures in mice and humans respectively (Figure 3A, 3B).

Microarray data from mouse neuronal forebrain (Sugino et al. 2006) was extracted from the Gene Expression Omnibus GDS1522 Accession number GSE2882. *In situ* hybridization data from mouse brain sections was extracted from the Allen Institute Brain Map (https://portal.brain-map.org). (Lein et al. 2007). RNAseq of mouse brain cell subtypes (www.brainrnaseq.org) (Zhang et al. 2014), mouse hippocampus RNAseq atlas (https://hipposeq.janelia.org) (Cembrowski et al. 2016) and 10X single cell RNAseq of mouse cortex and hippocampus (https://portal.brain-map.org/atlases-and-data/rnaseq/protocols-mouse-cortex-and-hippocampus) and human cortical cells (https://portal.brain-map.org/atlases-and-data/rnaseq/protocols-human-cortex) were extracted from the Allen Brain Map atlas (http://portal.brain-map.org). Supportive data was obtained from the Human protein atlas (www.proteinatlas.org Sjöstedt et al. 2020).

Cembrowski MS, Wang L, Sugino K, Shields BC, Spruston N. Hipposeq: a comprehensive RNA-seq database of gene expression in hippocampal principal neurons. *Elife*. 2016;5:e14997.

Lein ES, Hawrylycz MJ, Ao N, Ayres M, Bensinger A *et al*. Genome-wide atlas of gene expression in the adult mouse brain, *Nature* 2007;445:168-176.

Sjöstedt E, Zhong W, Fagerberg L, *et al*. An atlas of the protein-coding genes in the human, pig, and mouse brain. *Science*. 2020;367(6482) eaay5947.

Sugino K, Hempel CM, Miller MN, *et al*. Molecular taxonomy of major neuronal classes in the adult mouse forebrain. *Nat Neurosci*. 2006;9(1):99-107.

Zhang Y, Chen K, Sloan SA, *et al*. An RNA-sequencing transcriptome and splicing database of glia, neurons, and vascular cells of the cerebral cortex. *J Neurosci*. 2014;34:11929-47.